Study of the mask shape effect on the spatial distribution of GaAs layer growth rate in MOCVD selective area epitaxy

© A.E. Marichev, V.V. Shamakhov, A.E. Grishin, S.O. Slipchenko, N.A. Pikhtin

Ioffe Institute,
194021 St. Petersburg, Russia

E-mail: aemarichev@mail.ioffe.ru

Received October 14, 2025
Revised November 13, 2025
Accepted November 14, 2025

Within a numerical model of gas-phase diffusion, the influence of the shape (square, circle, rhomb) and size (from 2 to 10 μm) of masks on the spatial distribution of the GaAs layer growth rate in metal-organic chemical vapor deposition selective area epitaxy has been studied. It was found that the Growth Rate Enhancement (GRE) changes non-uniformly around the periphery of square-shaped mask windows: it is minimal at the center of the square's side and increases towards the vertices, with the maximum difference reaching 2.4 %. Reducing the GRE difference for a square window can be achieved by using a rhomb-shaped mask. The use of masks with circular windows ensures a minimal difference in GRE between the center and the edge with the growth rate uniform around the entire periphery. It is shown that the smallest difference in GRE between the window center and the edge can be observed with minimum mask-window widths and is 0.328 % for a circular window.

Keywords: simulation, gas-phase diffusion, selective area epitaxy, growth rate enhancement, windows, mask.

DOI: 10.61011/SC.2025.08.62598.8457

1. Introduction

Currently we see an active development of photonic integrated circuits requiring monolithic integration of active elements such as lasers, modulators, waveguides, and photodetectors [1–6]. Selective epitaxy can be one of the effective solutions to this problem [7,8]. Selective epitaxy is a controlled spatially localized epitaxial growing of a structure with the necessary parameters, combining the advantages of epitaxial growth and lithography. The principle of selective epitaxy is based on the creation of a pattern on a pre-prepared substrate consisting of open windows where the material is deposited and areas covered with a dielectric mask (for example, SiO_2), where, the material is not deposited under certain technological parameters (for example, reactor pressure and growth temperature) [9]. Selective growth consists of three processes. The particles of the substance that reach the window area undergo a pyrolysis reaction and participate in the growth of the epitaxial layer. The particles of the substance reaching the mask can either be adsorbed onto the surface of the mask and migrate to the window area due to surface diffusion, or desorbed from the surface of the mask in a short time. The desorbed particles return to the gas phase and, due to the resulting concentration gradient between the mask and the window, will diffuse in the gas phase towards the window. The selective growth process is determined by the total contribution of diffusion processes over the mask surface and diffusion in the gas phase [3]. These processes result in an increase in the growth rate relative to the growth rate of standard epitaxy on a planar surface without masks. At the same time, for the layers obtained by selective epitaxy, an inhomogeneous distribution of thickness and composition (in the case of triple or quadruple solid solutions) is formed over the area of the window [10,11]. Therefore, predicting the parameters of the layers obtained by selective epitaxy is an important task. The vapor phase diffusion model is used to predict the properties of layers obtained by selective epitaxy using the MOC hydride epitaxy technology [7,12]. This model is mainly used for endless strips with a window width from units to hundreds of micrometers [10,13,14], as well as square windows with a width of hundreds of micrometers [15]. Moreover, the diffusion in the vapour-phase is the dominant process for the method of MOC hydride epitaxy. This is due to the fact that the diffusion length in the gas phase reaches 100 micrometers, which is significantly longer than the surface diffusion length, which is units of micrometers [16,17]. Surface diffusion through the mask can contribute at mask widths commensurate with the length of the surface diffusion, i.e. units of micrometers. To account for it, the model must be supplemented with parameters, the value of which must be determined from experiments. Currently, such experimental parameters are not available. This article uses a model that was previously verified to describe growth during selective epitaxy in wide windows and demonstrated a fairly good agreement between the calculated results and experimental data [10].

This paper studied the distribution of the thickness of the GaAs layer in square and round windows with a width of 2 to 10 μm, limited by a mask with a width of 2 to 10 μm. The task was to identify patterns of thickness profile changes in order to obtain a minimum layer thickness difference between the center and the edge of the window. The smallest change in the profile of the layer thickness along the width of the window should make it possible to further

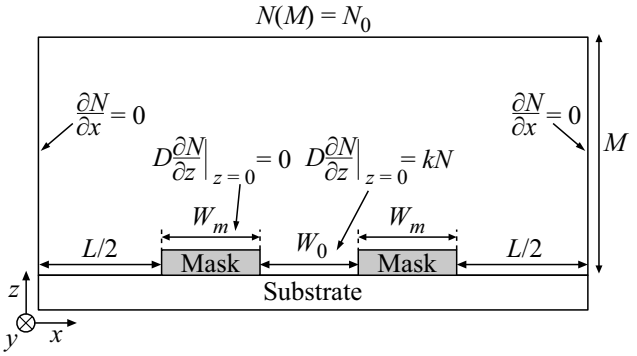

Figure 1. Schematic representation for a 3D model of vapour-phase diffusion, where k is the surface reaction constant; D is the diffusion coefficient of the precursor.

coordinate various elements of photonic integrated circuits with waveguides, as well as create the most favorable conditions for the growth of homogeneous active regions based on stressed quantum wells.

2. Vapour-phase diffusion model

The process of selective epitaxy, implemented within the framework of the technology of hydride epitaxy, can be described using the model of vapour-phase diffusion [18]. The model is based on the calculation of the concentration profile of matter particles in the gas phase above the substrate surface. The 3D distribution profile of the concentration of matter particles above the substrate is

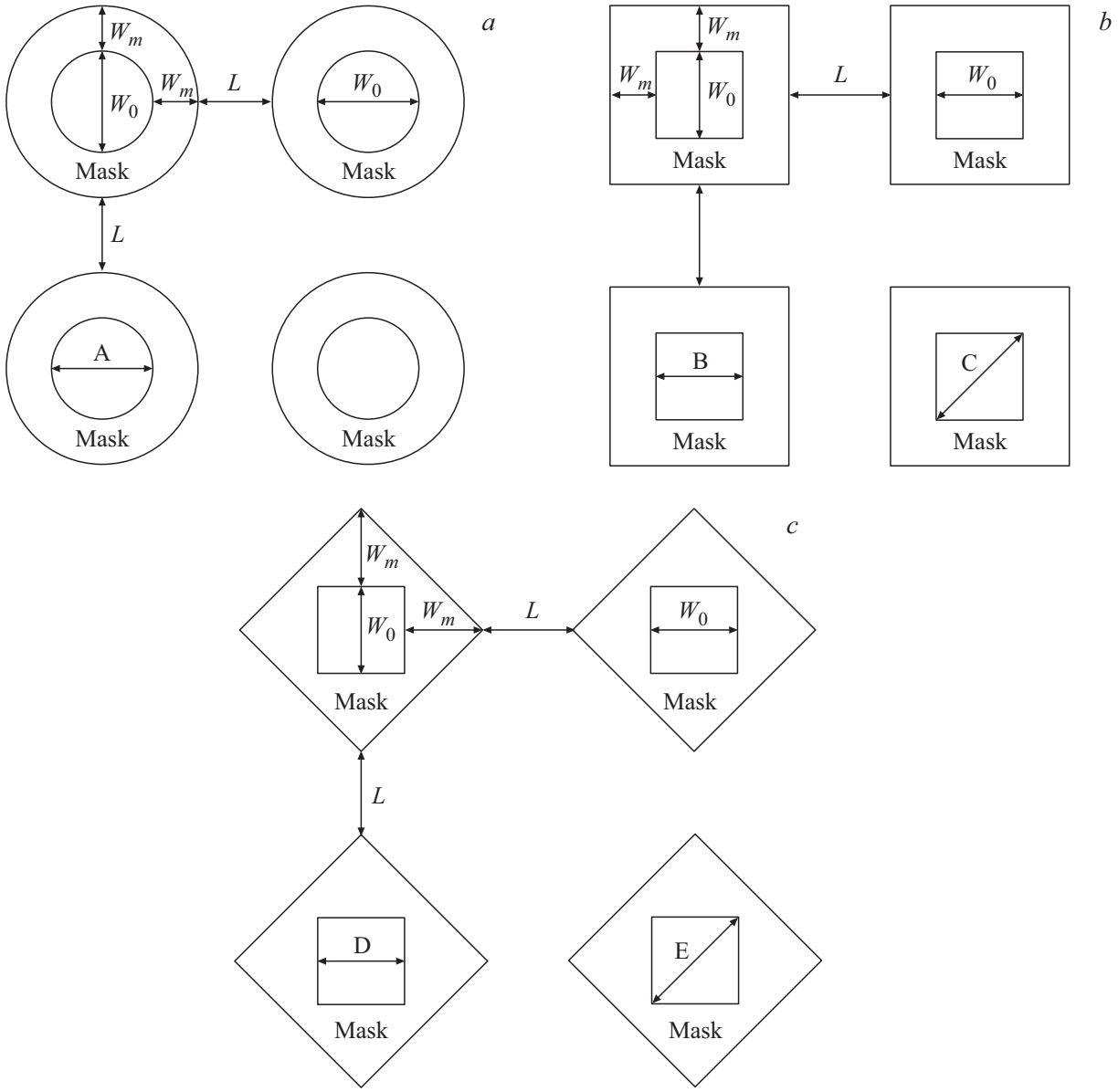

Figure 2. Configuration of the elements for calculating GRE: *a* — windows and masks in the form of a circle; *b* — windows and masks in the form of a square; *c* — windows in the form of a square and masks in the form of a diamond (a square rotated by 45°).

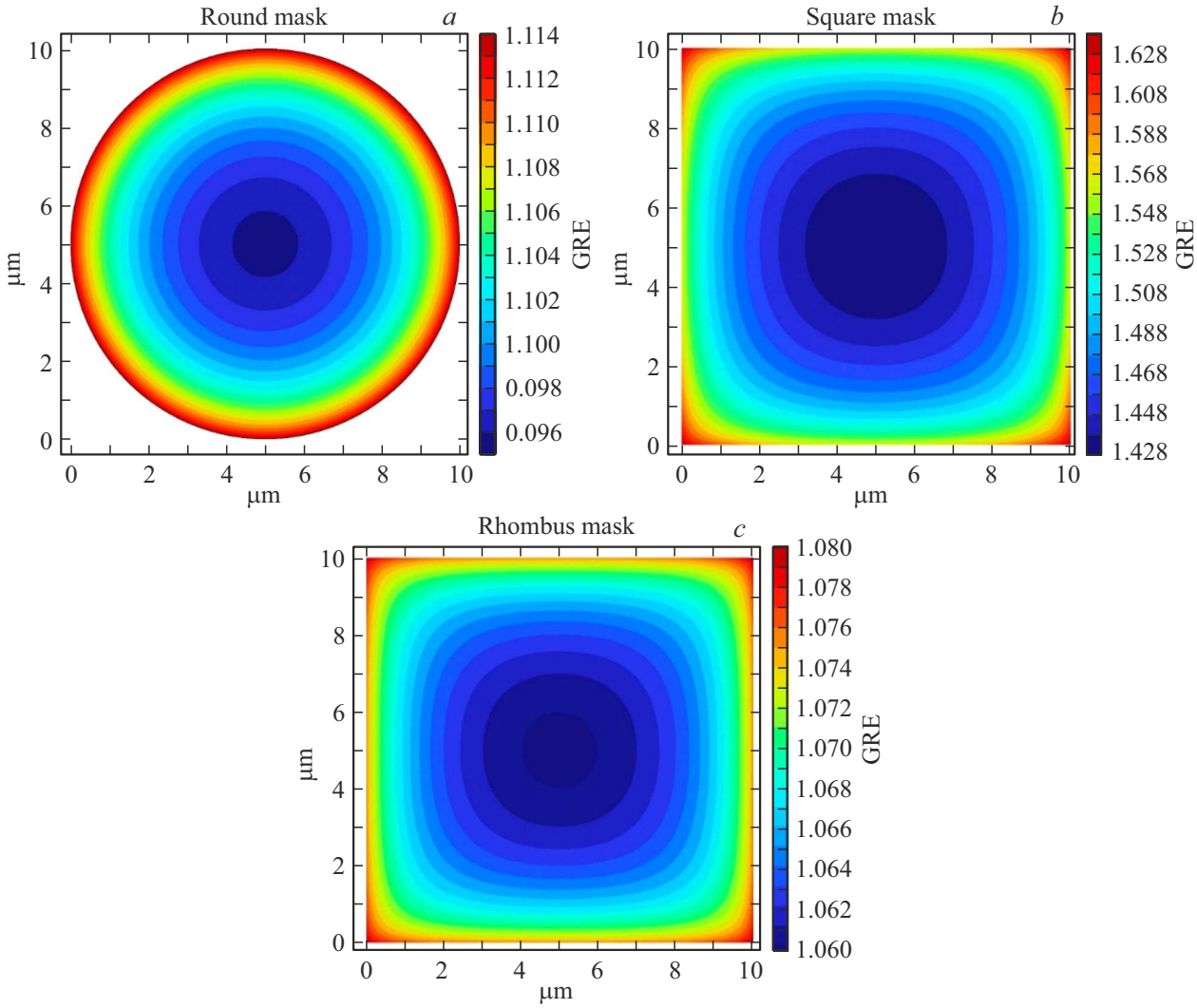

Figure 3. GRE calculation results with parameters W_0 and W_m equal to 10 μm for: *a* — windows and masks in the form of a circle; *b* — windows and masks in square-shaped windows; *c* — square-shaped windows and diamond-shaped masks.

determined by solving the Laplace equation in the boundary layer:

$$\frac{\partial^2 N}{\partial x^2} + \frac{\partial^2 N}{\partial y^2} + \frac{\partial^2 N}{\partial z^2} = 0, \qquad (1)$$

where N is the precursor concentration, x is the coordinate in the direction across the window, y is the coordinate in the direction along the window, z is the coordinate in the direction perpendicular to the plane of growth.

Figure 1 shows a diagram explaining the boundary conditions for calculating the selective epitaxy process within the framework of the vapour-phase diffusion model.

The boundary conditions at the edges of the window and the boundary layer can be written as follows (Figure 1):

– there is no growth on the surface of the mask:

$$\left.\frac{\partial N}{\partial z}\right|_{z=0} = 0; \qquad (2)$$

– the concentration of the precursor within the boundary layer does not change laterally:

$$\left.\frac{\partial N}{\partial x}\right|_{z=0} = 0; \qquad (3)$$

– the upper part of the boundary layer is located at a sufficiently large distance from the substrate to avoid disturbances introduced by the mask:

$$N(M) = N_0, \qquad (4)$$

where N_0 is the concentration of the precursor at the upper boundary of the boundary layer, which is constant;

– the growth process on an area without a mask is defined by the expression:

$$\left.\frac{\partial N}{\partial z}\right|_{z=0} = \frac{k}{D} N\Big|_{z=0}. \qquad (5)$$

The precursor concentration profile is determined by the parameter D/k, which can be considered as the effective

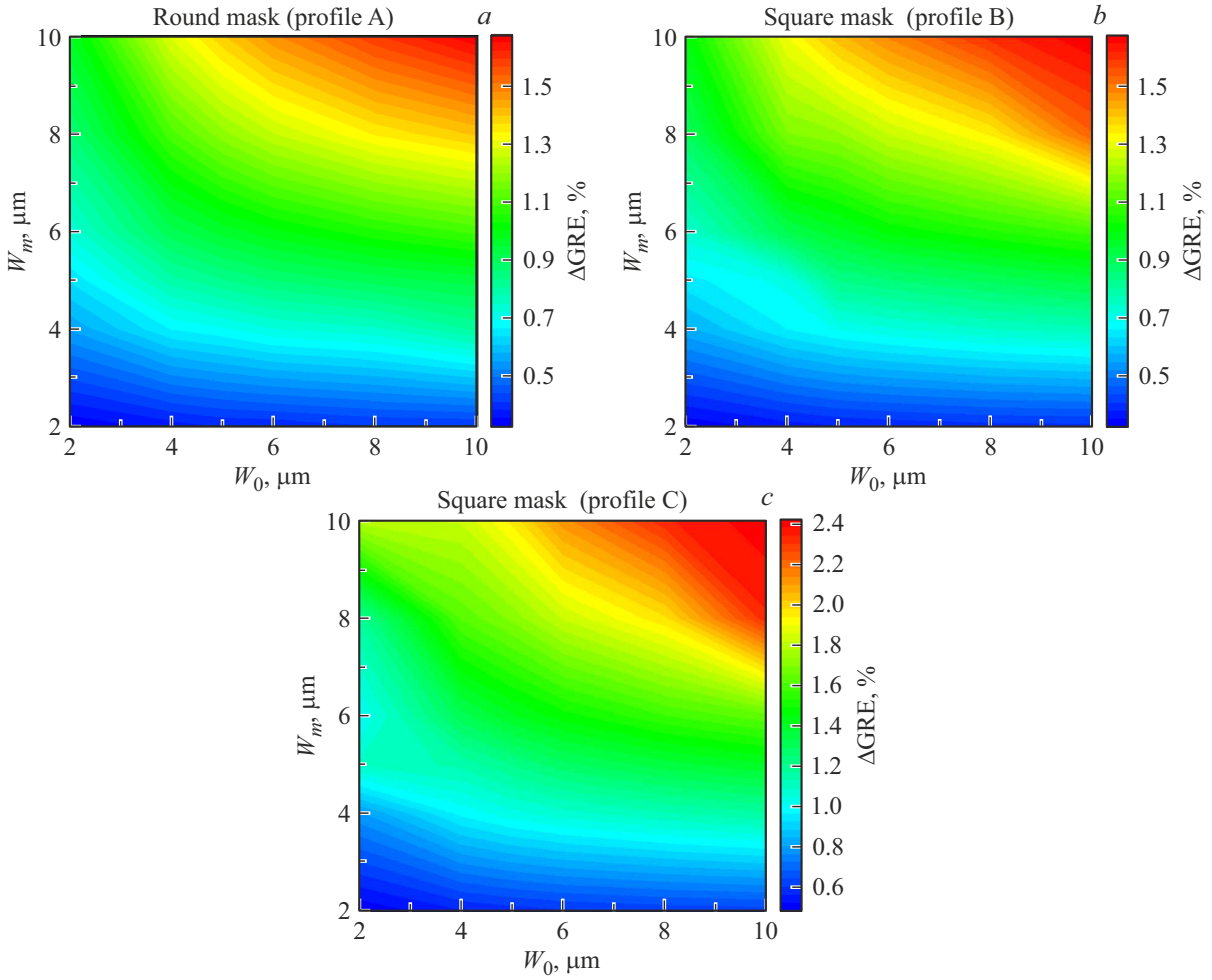

Figure 4. Change map of ΔGRE in the window depending on W_m and W_0: *a* — round window (section And in Figure 2, *a*); *b* and *c* — square window (sections B and C on Figure 2, *b*).

diffusion length. D/k can be estimated either by theoretical calculation [18], or by fitting an experimental result.

The concept of the growth rate enhancement (GRE) is used to estimate the growth rate profile of the layer grown in the mask window. GRE characterizes how the growth rate of a layer changes during selective epitaxy relative to the growth rate when deposited on a substrate without a mask. GRE is calculated according to the formula

$$\mathrm{GRE} = \frac{H}{H_p} = \frac{V}{V_p} = \frac{N}{N_0}\left(1 + \frac{M}{D/k}\right), \qquad (6)$$

where H and H_p is the thickness of the selectively grown layer and the standard grown layer, respectively; V and V_p is the speed of the selectively grown layer and the standard grown layer, respectively.

3. Modeling and discussion of the results

The modeling was performed for a group of separately round or square shaped elements bounded by a mask. The shape of the elements and masks is shown in Figure 2. The value L (the distance between adjacent figures) was taken to be $500\,\mu$m in the calculations in order to exclude the influence of the elements on each other. To analyze the effect of mask sizes, the values W_0 (window width) and W_m (mask width) were 2, 5 and $10\,\mu$m, the value $D/k = 85\,\mu$m for Ga [10].

The height of the boundary layer M was selected from the simulation results of the effect of the boundary layer height on GRE [10]. Thus, with an increase in the thickness of the boundary layer, there is a strong decrease in the effect of height on the maximum GRE. With a thickness of M greater than $1500\,\mu$m, the GRE does not change for masks 2/2, 5/5 and $10/10\,\mu$m.

Figure 3 shows the results of GRE calculations in round and square windows for GaAs. The figure shows that the minimum GRE value is at the center of the window, and as you approach the window/mask boundary, the GRE value increases. At the same time, for round windows (Figure 3, *a*), GRE is the same along the entire perimeter of the window. For a square window (Figure 3, *b*), the

GRE along the perimeter of the window varies from the minimum value in the center of the side of the square to the maximum value at the top of the square. And for a square window, the maximum GRE value is reached in the local areas corresponding to the vertices of the square. Thus, when forming stressed layers in a square window, the limiting factor is the GRE value at the vertices at the window/mask boundary.

To select the optimal ratio of W_0 and W_m, we analyzed the GRE variation between the window center and the window edge:

$$\Delta\mathrm{GRE} = \left|\frac{\mathrm{GRE}_0 - \mathrm{GRE}_1}{\mathrm{GRE}_0}\right| 100\,\%, \qquad (7)$$

where GRE_0, GRE_1 are the GRE values are in the center and at the edge of the window, respectively.

The most preferred option is when the GRE change between the center and the edge of the window is minimal. Figure 4 shows the ΔGRE change maps for round and square windows at different values W_0 and W_m. It can be seen from the maps that at a fixed value of W_m, the value of ΔGRE increases with increasing W_0. It can also be seen from the obtained maps that at a fixed value of W_0, the value of ΔGRE increases with increasing W_m. At the same time, ΔGRE has a stronger variation from W_m for larger windows (W_0). Thus, it is possible to conclude that the smallest change in ΔGRE occurs at the minimum values of W_0 and W_m. When comparing windows of different shapes, it can be seen that in a round window (Figure 4, *a*) ΔGRE is less than ΔGRE for a square window (Figure 4, *c*) between the center of the window and the vertex on the window/mask border. Therefore, from the point of view of obtaining more homogeneous layers, it is necessary to use a window and a mask in the form of a circle.

It can be seen from Figure 3, *b* and *c* that with the same window shape, the difference between the values of ΔGRE depends on the shape of the mask. So, for a diamond-shaped mask (Figure 3, *c*), the difference between *Delta*GRE in sections D and E (Figure 2, *c*) is less than the difference between ΔGRE in sections B and C (Figure 2, *b*) for a square mask (Figure 3, *b*). Thus, it can be concluded that when using a square-shaped window, the most preferable option is a diamond-shaped mask, i.e. a square rotated by 45° relative to the window.

4. Conclusion

The calculations performed within the framework of the vapour-phase diffusion model have shown that windows with a mask in the form of a circle are optimal compared to square windows and a mask, since the GRE change in such windows is minimal and uniform around the entire perimeter of the window, while for a square window the GRE changes along the perimeter inhomogeneously: minimally in the center of the side of the square and increases as you move towards the vertices of the square. It is also shown that the smallest GRE change between the window center and the edge is observed at the minimum values of window widths and masks.

Conflict of interest

The authors declare that they have no conflict of interest.

References

[1] P. Zhang. Proc. 4th Int. Conf. on Materials Chemistry and Environmental Engineering, **84** (1), 146 (2024).
[2] M.A. Butt, B. Janaszek, R. Piramidowicz. Sensors International, **6**, 100326 (2025).
[3] F. Lemaitre. Phd Thesis (Gonesse, Technische Universiteit Eindhoven, 2019).
[4] M. Smit, K. Williams, J. van der Tol. APL Photonics, **4**, 050901 (2019).
[5] B.M. Bersch, S.M. Eichfeld, Y.-C. Lin, K. Zhang, G.R. Bhimanapati, A.F. Piasecki, M. Labella, J.A. Robinson. 2D Mater., **4**, 025083 (2017).
[6] Y.-T. Lin, T.W. Yeh, P.D. Dapkus. Nanotechnology, **23**, 465601 (2012).
[7] J.D. Kim, X. Chen, J.J. Coleman. *Handbook of Crystal Growth*, 441–481 (2015).
[8] X. Yuan, D. Pan, Y. Zhou, X. Zhang, K. Peng, B. Zhao, M. Deng, J. He, H.H. Tan, C. Jagadish. Appl. Phys. Rev., **8** (2), 021302 (2021).
[9] G.J. Davies, W.J. Duncan, P.J. Skevington, C.L. French, J.S. Foord. Mater. Sci. Eng. B, **9** (1-3), 93 (1991).
[10] V. Shamakhov, S. Slipchenko, D. Nikolaev, I. Soshnikov, A. Smirnov, I. Eliseyev, A. Grishin, M. Kondratov, A. Rizaev, N. Pikhtin, P. Kop'ev. Technologies, **11** (4), 89 (2023).
[11] V. Shamakhov, S. Slipchenko, D. Nikolaev, A. Smirnov, I. Eliseyev, A. Grishin, M. Kondratov, I. Shashkin, N. Pikhtin. Nanomaterials, **13** (17), 2386 (2023).
[12] B. Wang, Y. Zeng, Y. Song, Y. Wang, L. Liang, L. Qin, J. Zhang, P. Jia, Y. Lei, C. Qiu, Y. Ning, L. Wang. Crystals, **12** (7), 1011 (2022).
[13] K.-L. Amaguchi, K. Okamoto. Jpn. J. Appl. Phys., **32**, 1523 (1993).
[14] M. Sugiyama. 22nd Int. Conf. on Indium Phosphide and Related Materials (IPRM), Kagawa, **1** (2010).
[15] T.M. Cockerill, D.V. Forbes, J.A. Dantzig, J.J. Coleman. IEEE J. Quant. Electron., **30** (2), 441 (1994).
[16] N. Dupuis, J. Décobert, P.-Y. Lagrée, N. Lagay, F. Poingt, C. Kazmierski, A. Ramdane, A. Ougazzaden. J. Appl. Phys., **103**, 113113 (2008).
[17] Xingyu Zhao, A.F. McKenzie, C.W. Munro, K.J. Hill, D. Kim, S.L. Bayliss, N.D. Gerrard, D.A. MacLaren, R.A. Hogg. J. Cryst. Growth, **603**, 127036 (2023).
[18] N. Dupuis, J. Decobert, P.Y. Lagreée, N. Lagay, C. Cuisin, F. Poingt, A. Ramdane, C. Kazmierski. IEE Proc. Optoelectron., **153** (6), 276 (2006).

Translated by A.Akhtyamov